

IMRT Treatment Planning Under Dose Uncertainty: A Polyhedral and Quadratic Programming Optimization Model

Atousa Arzanipour

PhD Student

Muma College of Business
University of South Florida

Tampa, FL, USA

arzanipour@usf.edu

Majid Rafiee

Chair and Associate Professor, Department of Industrial Engineering
Sharif University of University
Tehran, Tehran, Iran
rafiee@sharif.edu

Mehdi Mahnam

Assistant Professor, Department of Industrial Engineering
Isfahan University of Technology
Isfahan, Isfahan, Iran
m.mahnam@iut.ac.ir

Abstract

Cancer stands as a significant global mortality factor. Timely detection and proper treatment, such as intensity-modulated radiation therapy (IMRT), can hinder cancer progression. IMRT is crucial for targeting tumors while safeguarding healthy tissues. This study proposes a robust mathematical model addressing uncertainties in the dose delivered to the tumor as treatment sessions progress, using a polyhedral uncertainty set. The model employs linear constraints and a quadratic objective function derived from dose calculations. Variations of Newton-barrier and reduced gradient algorithms are utilized to solve the problem using real patient data, particularly from a prostate cancer case. Notably, the proposed method reduces penalties for healthy organs by approximately nine percent while maintaining an adequate dose delivered to the tumor.

Keywords

Optimization, Operations Research, IMRT, Cancer Treatment Planning, and Robust Optimization.

1. Introduction

Cancer is a type of disease in which specific cells in the body undergo abnormal proliferation. These newly created cells can also affect nearby cells and organs. Every year, cancer is the cause of death for ten million people (American Cancer Society, 2023). In 2025, it is estimated that cancer will cause the death of approximately 618,000 people in the United States alone (American Cancer Society 2024). However, if detected and treated early enough, the mortality

rate can be reduced. Cancer treatment planning typically includes radiation therapy, chemotherapy, and/or surgery (Bortfeld 2006). This research focuses primarily on radiation therapy, specifically intensity-modulated radiation therapy (IMRT), and associated mathematical programming. Radiation therapy is defined as a treatment in which the growth of cancerous cells and tissues is prevented using ionizing beams. These beams affect both healthy and cancerous cells; however, due to their intact DNA, healthy cells still retain the ability to reproduce. An effective treatment plan aims to deliver the desired dosage to the tumor while minimizing damage to healthy organs.

IMRT is an advanced form of radiation therapy that ensures targeted delivery of dosages to cancerous cells while minimizing damage to healthy tissues, achieved through the use of a linear accelerator. IMRT provides a high level of conformity between the shape of the planning target volume (PTV) and the radiation beams, especially when dealing with non-convex and complex PTV shapes. While IMRT improves treatment quality compared to other radiation therapy methods, it also increases the number of possible treatment plans and their corresponding parameters. Therefore, a trial-and-error approach is insufficient for developing a treatment plan, making inverse treatment planning necessary. In inverse treatment planning, the objective is to optimize all treatment plan parameters to maximize the effectiveness of the plan. As can be seen, this cannot be achieved without the help of optimization tools (Ehrhart et al. 2010).

The treatment planning process usually begins with a CT scan of the tumor area. Based on the CT scan images and different contouring of the tumor region and the nearby healthy organs, the treatment team calculates the dose strength pattern that best matches the tumor shape (Cancer Research UK, n.d.). The process of calculating the dose strength pattern is time-consuming and may take up to two weeks, so it is only done once at the start of the treatment.

Optimization can be helpful in various aspects of IMRT treatment planning, one of which is fluence map optimization. Fluence map optimization refers to the process of determining the most effective distribution of radiation intensity across the treatment area (Cho et al. 1998). In IMRT, several mathematical models have been developed, all of which are based on the concept of "discretization." To mathematically formulate the problems encountered in IMRT, each beam is divided into a set of beamlets or bixels. Additionally, within the patient's body, voxels (small volumetric elements) are defined to represent specific locations or coordinates; this is what discretization means (Rocha et al., 2012). Suppose we have $k=1, \dots, p$ beams, each with $j=1, \dots, n$ beamlets, and we have $i=1, \dots, m$ voxels. Then, D_{ijk} represents the amount of dose absorbed in voxel i from bixel j of the k^{th} beam. The standard model of IMRT for the dose absorbed by the i^{th} voxel in the target area, I , is as follows:

$$d_i = \sum_{j=1}^n D_{ij} x_j, \quad \forall i \subseteq I.$$

2. Literature Review

In the domain of IMRT, fluence map optimization has been studied more extensively than other sub-problems (Dias et al. 2016; Gao 2016; Ma et al. 2020; ten Eikelder et al. 2021; Zagorian et al. 2014). The first reason for this is that modeling the problem of fluence map optimization is more computationally tractable. The second reason is that an optimal fluence map has a higher impact on the overall quality of the treatment and can directly affect other aspects of IMRT, such as leaf sequencing (Men et al. 2007; Shepard et al. 2002). There are multiple ways to approach fluence maps: Physical or biological approaches, which focus on how doses are accumulated in the body or determining whether the map remains constant or changes throughout the treatment sessions. Additionally, we can incorporate uncertainty into the fluence map and examine how those uncertainties affect the quality of the treatment plan.

Biological models utilize biological concepts, such as the reaction of cells to radiation, as their basis. These models primarily focus on tumor control probability (TCP) or the probability of normal tissue complication (NTCP) (Thomas et al. 2005). On the other hand, physical models aim to define metrics and variables that facilitate the calculation of the dose received by each tissue. Many researchers have proposed linear mathematical formulations that incorporate constraints, such as a lower bound on the dose received by tumor cells or an upper bound on the dose received by healthy tissues or organs at risk (Romeijn et al. 2006). These constraints can also be integrated into the objective function. However, by employing nonlinear formulations, one can more accurately capture the reality of dose delivery to the patient's body. One highly popular objective function in nonlinear programming is the harmonic least squares, which aims to minimize the square of the difference between the prescribed dose and the received dose for healthy tissues, organs at risk, and tumorous regions (Wu & Mohan 2000). Depending on the significance of the healthy

organs, varying weights can be assigned to the squared difference, allowing for flexible prioritization. One metric used for evaluating physical dose is Dose-Volume Histograms (DVH) (Mukherjee et al. 2020). This histogram displays the percentage of each organ receiving a specific dose. In an ideal scenario, one hundred percent of the tumor volume should receive one hundred percent of the prescribed dose, and then the curve should have a steep slope approaching zero.

In IMRT treatment planning, fractionation is defined as dividing the prescribed dose, as determined by the medical team, into a series of daily dose deliveries. The purpose of fractionation is to allow normal tissues to recover from radiation exposure. The number of treatment sessions usually ranges from 25 to 35. In the literature, mathematical modeling of fluence maps delivered in each treatment session is categorized into two main areas: fixed or dynamic fluence maps. For example, in fixed fluence maps, if a dose of 50 grays is prescribed for the PTV, it will be administered over 25 sessions with a prescribed dose of 2 grays per session (50/25=2 grays); however, this constant prescribed dose is not the case for dynamic delivery of the dose.

The main rationale behind dynamic dose delivery in each session, along with its accompanying dynamic fluence maps, is to ensure maximum conformity to the treatment plan drafted by the medical team. Some research has demonstrated that dynamic fluence maps can also aid in reducing the deviation between the prescribed and delivered dose caused by uncertainties in the parameters (Ajdari & Ghate 2016). For instance, Nohadani et al. employed dynamic fluence maps to address uncertainties related to certain biological characteristics of tumors, such as the process of re-oxygenation (Nohadani & Roy 2017). Adibi et al.'s research has shown that utilizing dynamic fluence maps can result in a higher dose being delivered to the tumor (Adibi & Salari 2018). However, this might also be true for healthy organs. Gaddy et al. tackled this issue by using an optimization model in which an objective function penalizes deviations from the prescribed dose for these organs (Gaddy et al. 2019). Furthermore, many studies have explored the use of dynamic fluence maps in the simultaneous treatment of radiation therapy and chemotherapy (Salari et al. 2015).

In physical models with dynamic fluence maps, the value for the dose absorbed by the i^{th} voxel in the t^{th} session of the treatment is as follows:

$$d_{ti} = \sum_{j=1}^n D_{ij}x_{tj}, \quad \forall i \subseteq I, \forall t \subseteq L.$$

The use of mathematical programming in treatment planning offers numerous merits; however, the presence of uncertainties can hinder the planning process and potentially affect the quality of treatment. These uncertainties arise from the fact that each patient will react differently to the treatment. Some of the mentioned uncertainties include variations in the definition of the treatment region, such as gross tumor volume (GTV) or clinical target volume (CTV), uncertainties in the prescribed dose amount, uncertainties in the tolerance of healthy tissues and organs, and the most significant one: uncertainties in the amount of dose received by the patient due to setup errors or patient movement throughout the treatment session. Typically, in radiation therapy treatment, the approach to address uncertainties caused by the patient's movements is to incorporate 'Margins' like PTV so we can plan for a larger region, but this method is outdated due to its low accuracy (Biston et al. 2020). As a result, the development of probabilistic and robust optimization techniques has emerged as an alternative method to handle these uncertainties.

Stochastic optimization is commonly utilized when a distribution function can be assigned to the behavior of the uncertainty being dealt with. In IMRT treatment planning, stochastic programming can be used to optimize the expected value of squared penalty functions, the average value of TCP-based objective functions, or objective functions based on the average estimate of the accumulated dose (Bohoslavsky et al. 2013; Fontanarosa et al. 2013; Witte et al., 2007). In contrast, robust optimization methods are employed in cases where a distribution function for parameters with uncertainties cannot be defined, and only the minimum and maximum values of the parameters are known. The goal is to find a solution that is acceptable for all scenarios. In the context of IMRT, robust optimization techniques are usually employed to address uncertainties arising from organ movement due to patients' breathing and their various breathing patterns (P. Chan et al. 2008; T. C. Y. Chan et al. 2014).

To the best of our knowledge, despite the advantages of a dynamic treatment plan, not much research has been carried out on this subject due to the complexity of the solution space. While some previous literature exists on dealing with uncertainties in the parameters of biological models, patient movements (especially breathing movements), errors in

execution, and other factors, no research has so far focused on the gradual process of tumor shrinkage and its effect on the quality of treatment plans. Radiation therapy targets cancer cells by damaging their DNA, inhibiting their growth, and causing the tumor to gradually shrink in comparison to its original size, as observed in CT images. However, this shrinkage can pose challenges for treatment planning, as it necessitates adjustments to minimize harm to surrounding healthy tissues. Consequently, the focus of this research is to develop a treatment strategy capable of adapting to reductions in tumor size, thereby optimizing the quality of treatment plans.

In the first step, we develop a mathematical model of the problem that can yield multiple treatment plans during treatment sessions. This type of modeling, which is less discussed in the literature, aims to provide a treatment plan that closely adheres to the ideal treatment plan and is stable against changes in the tumor's shape. This ensures acceptable dose absorption by the tumor tissue while minimizing radiation absorption by healthy tissues and organs at risk. In the second step, we employ robust optimization approaches to create a robust counterpart for the non-deterministic lower limit allowed for the tumor after a certain number of sessions has progressed. This approach seeks to reduce the dose received by healthy tissues while ensuring the tumor receives the necessary dose.

3. Problem Formulation and Methods

Optimization techniques are highly utilized in IMRT treatment planning. Mathematical programming based on physical constraints has been widely used due to its linear space. This research introduces a mathematical model featuring a quadratic objective function and linear constraints. The primary aim is to minimize the radiation dose absorbed by healthy organs while ensuring that the tumor receives the necessary prescribed dose. As discussed in Section 2, during the treatment sessions, the proliferation of tumor cells gradually stops, leading to tumor shrinkage. This transformed tumor may require a different dosage, introducing the need for a lower limit for the tumor region. However, this lower limit is not a known and fixed value and can be considered a parameter with uncertainty. To address this uncertainty, we use a polyhedral uncertainty set and formulate a new robust counterpart.

3.1 Indices and Parameters

In this section, the key indices and parameters essential for understanding the presented formulation are introduced.

i	Index of the voxels of the treatment region (from 1 to m)
j	Index of the beamlets (from 1 to n)
t	Index of the treatment sessions (from 1 to q)
J	Set of beamlets
L	Set of treatment sessions
H	Set of healthy organs voxels
T	Set of tumor voxels
B	Set of treatment regions (includes two subsets T and H)
K	Set of healthy organs (from 1 to k)
N _{HK}	Total number of healthy organs
d _{pres}	The prescribed dose for tumor
U _j	The upper bound for the <i>j</i> th beamlet
TLB	The accepted lower bound for tumor
TUB	The accepted upper bound for tumor
D _{ij}	The amount of dose absorbed by the <i>i</i> th voxel from the unit beam radiated from the <i>j</i> th beamlet

3.3 Modeling the Deterministic Treatment Plan

Below, the basic formulation for the IMRT problem without any uncertainties is presented:

$$\min_x \sum_{k=1}^K \left(\frac{1}{N_{H_k}} \sum_{t=1}^q \sum_{i \in H_k} (d_{ti})^2 \right)$$

$$TLB \leq d_{ti} \quad \forall i \in T, \forall t \in L \quad (1)$$

$$d_{ti} \leq TUB \quad \forall i \in T, \forall t \in L \quad (2)$$

$$0 \leq x_{jt} \leq U_j \quad \forall j \in J, \forall t \in L \quad (3)$$

The objective function aims to minimize the gap between the received dose by the patient and the ideal prescribed dose for healthy organs, which is zero. This quadratic objective function is a common choice in the literature of fluence map mathematical modeling problems. Constraints 1 and 2 establish the lower and upper dose boundaries for the tumor. These boundaries, denoted by TLB and TUB respectively, ensure that each tumor cell receives a minimum dose while avoiding excessive exposure. Furthermore, Constraint 3 sets the non-negativity and upper limit for x_{jt} , ensuring the overall treatment optimization.

3.4 Modeling the uncertainty and the robust counterpart

As previously mentioned, as the treatment sessions progress, the proliferation of tumor cells is anticipated to stop, necessitating the consideration of a new treatment plan. Typically, treatment sessions are initially designed based solely on the information obtained from the first CT scan. However, leveraging optimization tools enables us to re-calibrate the treatment sessions without requiring additional inputs, such as a secondary CT scan. In a study conducted by Nohadani et al., it was observed that after one-third of the sessions have passed, the initial information of the system derived from cell reactions in the treatment section changes to a point where the initial treatment plan may no longer be optimal (Nohadani & Roy 2017). Consequently, in this research, a new lower bound for the tumor is determined after one-third of the sessions. Recognizing the uncertainty associated with this value, we define it as an uncertainty parameter. Consequently, constraint 1 is transformed into constraints 4 and 5.

$$TLB \leq d_{ti} \quad \forall i \in T, \forall t \leq \left\lfloor \frac{q}{3} \right\rfloor \quad (4)$$

$$\widetilde{TLB} \leq d_{ti} \quad \forall i \in T, \forall t \geq \left\lfloor \frac{q}{3} \right\rfloor + 1 \quad (5)$$

\widetilde{TLB} is the uncertain parameter we have here serving as the lower bound for the tumor area in the final two-thirds of the sessions. To construct the robust counterpart of this constraint, with the help of a new variable $y_0 = -1$, \widetilde{TLB} is moved to the left-hand side of the constraint. As a result, constraint 5 will be transformed into the following form of the constraint.

$$\left\{ -d_{ti} - \widetilde{TLB}y_0 \leq 0 \quad \forall i \in T, \forall t \geq \left\lfloor \frac{q}{3} \right\rfloor + 1 \quad y_0 = -1 \right.$$

\widetilde{TLB} is equal to $TLB + \epsilon \widetilde{TLB}$. Here, TLB represents the nominal value of the parameter, \widetilde{TLB} represents positive constant perturbation, and ϵ is an independent random variable corresponding to uncertainty. Therefore, we can substitute the expression for \widetilde{TLB} with $TLB + \epsilon \widetilde{TLB}$ in the set of constraints mentioned above:

$$\left\{ -d_{ti} - TLBy_0 - \epsilon \widetilde{TLB}y_0 \leq 0 \quad \forall i \in T, \forall t \geq \left\lfloor \frac{q}{3} \right\rfloor + 1 \quad y_0 = -1 \right.$$

In the robust optimization approach, the goal is to find a solution that is feasible for all values of ϵ so the uncertainty set would be safe against all in-feasibility. Meaning:

$$\left\{ -d_{ti} - TLBy_0 - \max(\epsilon \widetilde{TLB}y_0) \leq 0 \quad \forall i \in T, \forall t \geq \left\lfloor \frac{q}{3} \right\rfloor + 1 \quad y_0 = -1 \right.$$

The decision regarding the space of ϵ can be reflected in the formulation of the robust counterpart. To write the robust counterpart of this problem, we have used a polyhedral uncertainty set. This approach was first introduced by Bertsimas and Sim, and one of its main advantages is the linearity of its uncertain space formulation. The polyhedral uncertainty set is defined as follows:

$$U_1 = \{ \epsilon \mid \sum_j |\epsilon_j| \leq \tau \}$$

In which τ is an adjustable parameter that will define the size of the uncertainty set. So, the robust counter part of the set would be:

$$\begin{aligned}
 -d_{ti} + TLB + z\tau &\leq 0 \quad \forall i \in T, \forall t \geq \lfloor \frac{q}{3} \rfloor + 1 \\
 z &\geq \widehat{TLB}
 \end{aligned}$$

Here, z is a decision variable introduced into our problem, with its value always constrained to be less than the positive constant perturbation of the uncertain parameter. Thus, the formulation of our problem, along with its robust counterpart, can be summarized as follows:

$$\begin{aligned}
 \min_x \sum_{k=1}^K & \left(\frac{1}{N_{H_k}} \sum_{t=1}^q \sum_{i \in H_k} (d_{ti})^2 \right) \\
 d_{ti} = \sum_{j=1}^m & D_{ij} x_{jt}, \quad \forall i \in B, \forall t \in L \\
 TLB \leq d_{ti} & \quad \forall i \in T, \forall t \leq \lfloor \frac{q}{3} \rfloor \\
 -d_{ti} + TLB + z\tau &\leq 0 \quad \forall i \in T, \forall t \geq \lfloor \frac{q}{3} \rfloor + 1 \\
 z &\geq \widehat{TLB} \\
 d_{ti} \leq TUB & \quad \forall i \in T, \forall t \in L \\
 0 \leq x_{jt} \leq U_j & \quad \forall j \in J, \forall t \in L
 \end{aligned}$$

3.5 Methodology

In fluence map optimization problems, usually, each voxel is considered as a decision variable, making the problem both large and complicated. For instance, in the case study presented in Section 5, there are approximately 26,000 voxels, and therefore, decision variables, for the target region. The complexity is further heightened by considerations of dynamic fluence maps and uncertainties. Adding to the challenge, our problem formulation involves a quadratic objective function. Given these factors, it becomes evident that there is a need for algorithms that can expedite the process of finding the optimal solution since using regular methods such as Simplex may consume significant time and computing resources. To address problems with a convex and linear feasible region and a quadratic objective function, several algorithms exist to aid in speeding up the process. In this research, we have chosen to utilize the Newton-barrier method implemented in GAMS/XPRESS and the Reduced Gradient algorithm implemented in GAMS/MINOS.

3.5.1 Newton-barrier Method

The Simplex method, widely used for solving linear programming problems, searches through the boundary points in order to find a better solution. However, this is opposite for Newton-barrier algorithms, where the search is highly focused on only the internal points or vertices of the feasible region. Most of the time, it will be able to find only an approximation of the optimal solution due to some degree of non-linearity in the feasible region or objective function.

The algorithm begins by initializing a set of x_0 . Subsequently, the constraints' values are computed, and if they are not satisfied, a new function called the Barrier function is introduced. The purpose of this function is to penalize x values that violate the constraints. The severity of these penalties can vary based on an internal parameter we denote as t . Subsequently, this barrier function is incorporated into the objective function. The resultant objective function $F(x)$ becomes:

$$F(x) = f(x) + tB(x)$$

Where $B(t)$ is the barrier function and $f(x)$ is the initial objective function. In the subsequent step, Newton's method is employed to minimize the new objective function, $F(x)$. The updated x is calculated as follows:

$$x_{k+1} = x_k - [\nabla^2 F(x_k)]^{-1} \nabla F(x_k)$$

The optimization process will continue until the changes in x_{k+1} and x_k become sufficiently small. This method, known as the Newton-barrier method, is implemented in the commercial optimization solver GAMS under the name XPRESS (FICO, n.d.).

3.5.2 Reduced Gradient method

When the non-linearity of the problem lies only in the objective function and all the constraints are in their linear form, the solver GAMS/MINOS uses a reduced-gradient algorithm, first introduced by Wolfe, combined with a quasi-Newton algorithm (Murtagh & Saunders, 1978). In the reduced gradient method, the set of constraints $Ax + Is = 0$ is transformed into:

$$Bx_B + Sx_S + Nx_N = 0$$

Where x_S is the set of super-basic variables and x_B and x_N are sets of basic and non-basic variables, respectively. For every solution, usually, super-basic and basic variables stay within their bounds while the non-basic variables have a value of zero. When both the objective function and the constraints are linear, the reduced-gradient method works in the same manner as the simplex method, where the goal of moving variables is to reduce in-feasibility or improve the objective function value.

In the reduced-gradient algorithm provided by GAMS/MINOS, a quasi-Newton algorithm is implemented to optimize the super-basic variables. Consider Z as below (General Algebraic Modeling System (GAMS), 1992):

$$(-B^{-1}S \ I \ 0).$$

The search direction q can be calculated using the formulation:

$$R^T Rq = -Z^T g$$

Where g is the gradient of the non-linear part of the objective function and R is an upper triangular matrix. Once q is found, the search direction for all variables is defined as $p = Zq$. This process will continue until the reduced gradient of the objective function is sufficiently close to zero, typically 10^{-6} . This variation of the reduced-gradient method is implemented and can be found in a solver named GAMS/MINOS.

4. Data Collection

To analyze the effectiveness of the proposed model in Section 3, we will use a real-world dataset from the 'Common Optimization for Radiation Therapy (CORT)' project (Craft et al., 2014). This data set, obtained from Massachusetts General Hospital, includes multiple cases. For this research, we have chosen a patient undergoing prostate cancer treatment from the CORT dataset. Figure 1, sourced from the dataset's research paper, shows a CT scan image of the patient with prostate cancer. Colored lines delineate all essential tissues for planning. PTV-68 represents the primary tumor region in the prostate, while PTV-56 includes a portion of the tumor region and the lymph nodes. Other tissues exposed to radiation include the bladder, left and right femoral heads, rectum, and the surrounding healthy tissues of PTV-68 and PTV-56.

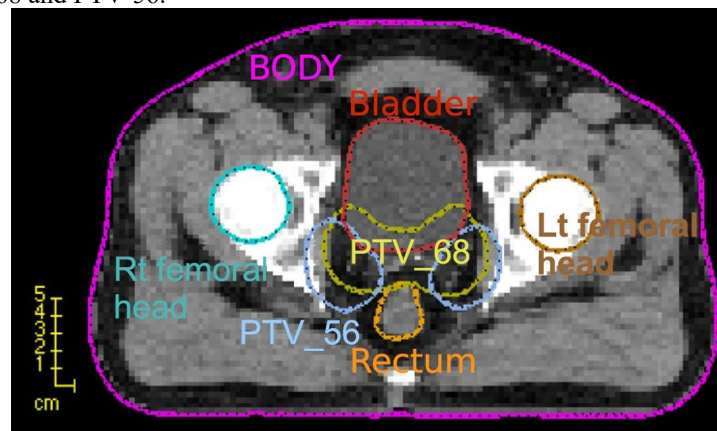


Figure 1. Different regions for prostate cancer patient

The proposed robust mathematical model was solved using both Newton-barrier and reduced-gradient methods on a computer with 16 cores and 16 gigabytes of RAM. These methods, available as solvers in GAMS under the names XPRESS and MINOS, can be customized by adjusting their parameters.

For this research, the default settings of these solvers were utilized. Table 1 lists the values of all parameters chosen for the prostate cancer problem. Additionally, Table 2 presents the values required for the robust counterpart of this problem.

Table 1. Input values for the problem parameters

Parameter	Value
Number of beams' directions	5 angles
Number of beamlets in all angles	863
Number of treatment sessions	34
Number of tumor's voxels	6770
Number of bladder's voxels	11596
Number of femoral heads' voxels	5957
Number of rectum's voxels	1764
The allowed lower bound for tumor in each session	$95\% \times 2 = 1.9$
The allowed upper bound for tumor in each session	$107\% \times 2 = 2.14$
Maximum beam intensity for the j^{th} beamlet	50

Table 2: Input values for the problem robust parameters

Parameter	Value
Minimum value for $\widehat{T\overline{L}B}$	1
Maximum value for $\widehat{T\overline{L}B}$	1.9
Value of τ	0.8
$\widehat{T\overline{L}B}$	0.45

5. Results and Discussion

With the mentioned inputs in Table 1, the model was solved using reduced gradient and Newton Barrier methods, and a summary of the computation time and results for both methods is shown in Table 3.

5.1 Numerical Results

By examining Table 3, it can be deduced that the proposed radiation delivery method in this research successfully achieved a lower value for the objective function. This indicates that healthy organs received a lower dosage compared to the fixed fluence map method, which does not account for re-planning for the tumor.

Table 3. Computation time and results for NB and RG methods.

	NB	RG
CPU time (in minutes)	212	65
Number of Iterations	51	72
Objective function value in the basic state	3251	3251
Objective function value in the robust state	2942	2942

Table 4. The percentage of the bladder receiving specific dosage.

	25 Gy	40 Gy	64 Gy
% of Volume (Base)	51	36	17
% of Volume (Robust)	49	34	11

Table 5. The percentage of the rectum receiving specific dosage.

	32 Gy	40 Gy	50 Gy
% of Volume (Base)	55	55	27
% of Volume (Robust)	49	49	23

Table 6. The percentage of the femoral head receiving specific dosage.

	15 Gy	20 Gy	25 Gy
% of Volume (Base)	34	22	8
% of Volume (Robust)	29	19	6

5.2 Graphical Results

The solution of a 3-D treatment plan comprises numerous outputs, and sometimes interpreting these outputs can be challenging. One way to address this issue is through the use of Dose-Volume Histograms (DVHs). DVHs summarize the dose distribution in the treatment region and the tissues surrounding the tumor, which is of high importance. In DVHs, the horizontal axis typically shows the amount of dose in Grays, and the vertical axis shows the percentage of a specific organ receiving that dose. In this study, DVHs are utilized for two primary objectives: the first is to verify whether the tumor region is receiving the required dose, and the second is to evaluate the radiation absorbed by healthy organs.

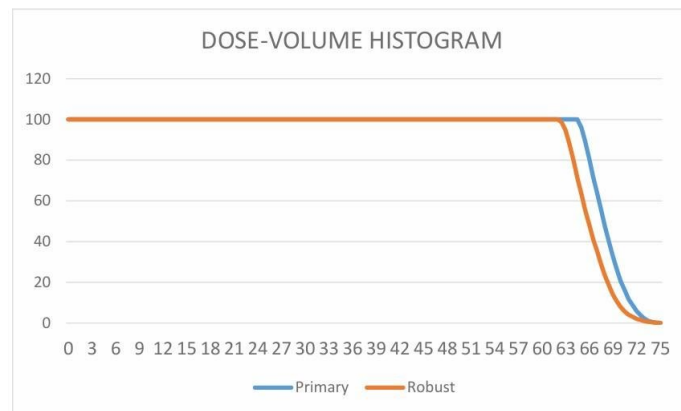


Figure 2. Dose-Volume histogram for tumor region

Figure 3 shows the dose-volume histograms of healthy organs, including the bladder, rectum, and the left femoral head. Tables 5, 6 and 7 compare the dosage received by healthy organs in the proposed method with that in the base method. In the case of the bladder, there was a 54% reduction in the volume exposed to 64 Grays. This same pattern

is observed with other healthy organs as well. Reducing radiation exposure to healthy organs can lower the risk of genitourinary and gastrointestinal toxicities for prostate cancer patients, and the reductions observed in this case may help mitigate that risk as well.

By examining the figures and tables, we can observe that transitioning from a fixed treatment plan to allowing replanning of treatment sessions significantly reduces the dosage delivered to the healthy organs of the bladder and rectum. Additionally, there is a less significant but still positive effect on the femoral heads. For example, according to Table 7, in the robust method, the femoral head receives 14.7% less exposure to doses exceeding 15 Grays and 25% less exposure to 25 Grays.

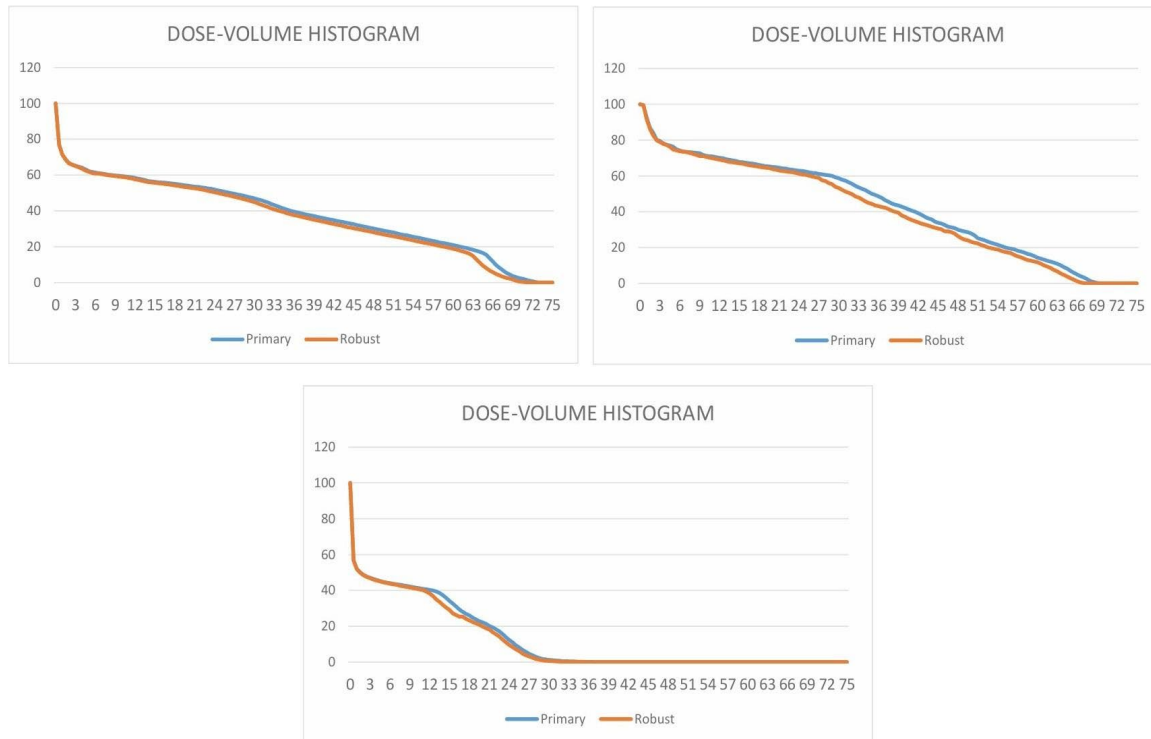


Figure 3. Dose-Volume histograms for bladder (top-left), rectum (top-right) and femoral head (bottom-center)

5.3 Proposed Improvements

The results indicate that even when the dose received by the healthy organ is reduced, the tumor still obtains a significant percentage of its prescribed dose, as illustrated in Figure 2. In the fixed fluence map method, 95% of the tumor region receives 65 Grays, with the entire tumor receiving 64 Grays. After implementing the proposed method on this dataset, we observed a lower dose absorption by the tumor. However, despite the reduced dose absorbed by healthy organs, the tumor still received a substantial amount of its required radiation. According to Table 4, 94 percent of the tumor received 92.6 percent of the prescribed dose. Table 4 also details the percentage of the tumor volume that received specific doses relative to the prescribed amount.

Table 7. The percentage of the tumor receiving different fractions of the prescribed dosage.

	94%	96%	98%
% of Volume (Base)	100	89	80
% of Volume (Robust)	87	63	48

By looking at Figure 2, it can be observed that in the base method, 95% of the prescribed dose, which is 64 Gy, was received by one hundred percent of the tumor, while in the proposed robust method, 91% of the prescribed dose was received by 100% of the tumor.

Figure 3 shows the dose-volume histograms of healthy organs, including the bladder, rectum, and the left femoral head. Tables 5, 6 and 7 compare the dosage received by healthy organs in the proposed method with that in the base method. In the case of the bladder, there was a 54% reduction in the volume exposed to 64 Grays. This same pattern is observed with other healthy organs as well.

By examining the figures and tables, we can observe that transitioning from a fixed treatment plan to allowing replanning of treatment sessions significantly reduces the dosage delivered to the healthy organs of the bladder and rectum. Additionally, there is a less significant but still positive effect on the femoral heads. For example, according to Table 7, in the robust method, the femoral head receives 14.7% less exposure to doses exceeding 15 Grays and 25% less exposure to 25 Grays.

5.4 Sensitivity Analysis

This model was only tested on one case of a patient going through prostate cancer but in order to make sure that the model is working and can be generalized, a sensitivity analysis is done on the uncertainty parameter. τ shows the level of conservatism and Figure 4 illustrates the impact of different τ values (ranging from zero to one) on the objective function. As expected, increasing τ leads to greater conservatism, which compromises the optimality of the objective function while ensuring feasibility.



Figure 4. Sensitivity analysis of the outcomes to different values of τ

6. Conclusion

One out of every six deaths is attributed to cancer. However, when cancer is accurately diagnosed and treated early, its mortality rate can be significantly reduced. Radiation therapy, a prominent cancer treatment, stops tumor cell growth by damaging DNA, yet its timing and mechanism remain unclear. In this study, this observation is exploited to devise a novel treatment strategy, aiming to target tumors effectively while sparing healthy tissues. Employing mathematical modeling, a linear model with a quadratic objective function is introduced, and then the Newton-barrier and reduced gradient methods are used for solving the proposed model. Validating our model with a case study on prostate cancer, results are presented via dose-volume diagrams for thorough evaluation. The key outcomes of this research are as follows:

Regarding tumor control, the results show that the proposed model effectively controls tumor growth throughout the sessions, ensuring the accurate delivery of the required dose. Notably, 80 percent of the tumor still receives 95 percent of the intended dose, indicating the model's capability to achieve precise targeting and successful dose delivery to the tumor while safeguarding healthy tissues from excessive radiation.

Another primary objective of this research was to mitigate excessive radiation exposure to healthy organs. Figure 3 clearly demonstrates that the proposed model significantly reduces the dose received by healthy tissues in the bladder, rectum, and femoral heads. This reduction effectively prevents potential damage to the DNA of these organs. By

carefully controlling the radiation distribution, the proposed model prioritizes the protection of healthy tissues while delivering the required dose to the tumor site. This aspect of the model contributes to enhancing the safety and overall effectiveness of radiation therapy treatment. The objective functions in both the basic model and the proposed model of this problem are defined as the summation of average penalties for the dose received by each voxel in healthy tissue, measured against the ideal state where the recommended dose is zero. Based on the results, there is a significant reduction in penalties, resulting in a 9.2 percent improvement in the objective function aimed at minimizing fines. Consequently, the proposed model demonstrates superior performance in optimizing the treatment plan and reducing potential harm to healthy tissues, making it a more effective and efficient approach for radiation therapy.

This research has introduced a dynamic fluence map as a solution to address the inflexibility observed in treatment plans using a fixed fluence map. The variable fluence map allows for potential rescheduling of certain parameters after one-third of the treatment sessions have been completed, without the need for new inputs that could slow down the treatment schedule. In future research, it would be interesting to explore treatment plans that can be re-programmed multiple times while maintaining the same procedure. This could involve investigating how changes in the system after secondary programming might necessitate further reprogramming. Identifying these critical points and developing models to address them could be a promising area of study for expanding research in this field. Additionally, researchers can also consider setup errors and patients' movement during the session as factors influencing tumor shrinkage and the need for re-planning.

The International Commission on Radiation Units and Measurements (ICRU) guidelines aim to ensure adequate tumor coverage and dose uniformity. For example, the guideline for tumor region is that the prescribed dose should cover at least 95% of the PTV, balancing efficacy and safety. In this research this dose level is slightly below traditional ICRU recommendations. Robust optimization prioritizes maintaining target coverage under a range of anatomical and setup uncertainties, potentially improving overall treatment reliability. Furthermore, partial underdosage may be acceptable if the dose distribution remains within clinically validated thresholds and tumor control probability is not significantly compromised. Ultimately, this trade-off reflects a shift from idealized static plans to more realistic and resilient treatment strategies. However advanced models can be studied to see the effect of more re-planning on the fact of tumor underdosing.

This study focuses on fluence map optimization but the proposed re-planning approach after one-third of treatment sessions can be extended to other radiation therapy problems, such as joint optimization of fluence maps with beam angles, sequencing (DAO), and VMAT. Fluence map optimization is particularly challenging due to its scale—spanning millions of voxels—and the added complexity of session-specific variability. To manage this, the study uses a polyhedral uncertainty set. Future work could explore alternative uncertainty models, such as ellipsoidal, box, or hybrid sets, to assess their impact on planning performance.

References

Adibi, A., & Salari, E. , Spatiotemporal radiotherapy planning using a global optimization approach. *Physics in Medicine & Biology*, 63(3), 035040 , (2018). . <https://doi.org/10.1088/1361-6560/aaa729>

Ajdari, A., & Ghate, A. , Robust spatiotemporally integrated fractionation in radiotherapy. *Operations Research Letters*, 44(4), 544–549, (2016). . <https://doi.org/10.1016/j.orl.2016.05.007>

American Cancer Society. ,*American Cancer Society Releases Latest Cancer Statistics, Launches Initiative to Address Prostate Cancer Resurgence and Disparities*, (2023).

American Cancer Society. , 2025 *Cancer Facts and Figures*, (2024). . <https://www.cancer.org/content/dam/cancer-org/research/cancer-facts-and-statistics/annual-cancer-facts-and-figures/2025/2025-cancer-facts-and-figures-acrs.pdf>

Biston, M.-C., Chiavassa, S., Grégoire, V., Thariat, J., & Lacornerie, T. , Time of PTV is ending, robust optimization comes next. *Cancer/Radiothérapie*, 24(6–7), 676–686, (2020). . <https://doi.org/10.1016/j.canrad.2020.06.016>

Bohoslavsky, R., Witte, M. G., Janssen, T. M., & van Herk, M. , Probabilistic objective functions for margin-less IMRT planning. *Physics in Medicine and Biology*, 58(11), 3563–3580. <https://doi.org/10.1088/0031-9155/58/11/3563>

Bortfeld, T. , IMRT: a review and preview. *Physics in Medicine and Biology*, 51(13), R363–R379, (2006). . <https://doi.org/10.1088/0031-9155/51/13/R21>

Cancer Research UK. (n.d.). *Your radiotherapy planning appointment*.

Chan, P., Dinniwell, R., Haider, M. A., Cho, Y.-B., Jaffray, D., Lockwood, G., Levin, W., Manchul, L., Fyles, A., & Milosevic, M. (2008). Inter- and Intrafractional Tumor and Organ Movement in Patients With Cervical Cancer Undergoing Radiotherapy: A Cinematic-MRI Point-of-Interest Study. *International Journal of Radiation Oncology*Biology*Physics*, 70(5), 1507–1515. <https://doi.org/10.1016/j.ijrobp.2007.08.055>

Chan, T. C. Y., Mahmoudzadeh, H., & Purdie, T. G. , A robust-CVaR optimization approach with application to breast cancer therapy. *European Journal of Operational Research*, 238(3), 876–885.(2014). <https://doi.org/10.1016/j.ejor.2014.04.038>

Cho, P. S., Lee, S., Marks, R. J., Oh, S., Sutlief, S. G., & Phillips, M. H. , Optimization of intensity modulated beams with volume constraints using two methods: Cost function minimization and projections onto convex sets. *Medical Physics*, 25(4), 435–443, 1998. <https://doi.org/10.1118/1.598218>

Craft, D., Bangert, M., Long, T., Papp, D., & Unkelbach, J. , Shared data for intensity modulated radiation therapy (IMRT) optimization research: the CORT dataset. *Gigascience*, 3(1), 2014. <https://doi.org/10.1186/2047-217X-3-37>

Dias, J., Rocha, H., Ventura, T., Ferreira, B., & Lopes, M. do C. , Automated fluence map optimization based on fuzzy inference systems. *Medical Physics*, 43(3), 1083–1095, 2016. <https://doi.org/10.1118/1.4941007>

Ehrgott, M., Güler, Ç., Hamacher, H. W., & Shao, L. , Mathematical optimization in intensity modulated radiation therapy. *Annals of Operations Research*, 175(1), 309–365, 2010. <https://doi.org/10.1007/s10479-009-0659-4>

FICO. (n.d.). *FICO Xpress Optimization Documentation*.

Fontanarosa, D., van der Laan, H. P., Witte, M., Shakirin, G., Roelofs, E., Langendijk, J. A., Lambin, P., & van Herk, M. (2013). An in silico comparison between margin-based and probabilistic target-planning approaches in head and neck cancer patients. *Radiotherapy and Oncology*, 109(3), 430–436, 2013. <https://doi.org/10.1016/j.radonc.2013.07.012>

Gaddy, M. R., Unkelbach, J., & Papp, D. (2019). Robust spatiotemporal fractionation schemes in the presence of patient setup uncertainty. *Medical Physics*, 46(7), 2988–3000. <https://doi.org/10.1002/mp.13593>

Gao, H. , Robust fluence map optimization via alternating direction method of multipliers with empirical parameter optimization. *Physics in Medicine and Biology*, 61(7), 2838–2850, 2016. <https://doi.org/10.1088/0031-9155/61/7/2838>

General Algebraic Modeling System (GAMS). (1992). *MINOS 5.5 User Manual*.

Ma, L., Chen, M., Gu, X., & Lu, W., Deep learning-based inverse mapping for fluence map prediction. *Physics in Medicine & Biology*, 65(23), 2020, 235035. <https://doi.org/10.1088/1361-6560/abc12c>

Men, C., Romeijn, H. E., Taşkin, Z. C., & Dempsey, J. F. , An exact approach to direct aperture optimization in IMRT treatment planning. *Physics in Medicine and Biology*, 52(24), 7333–7352, 2007. <https://doi.org/10.1088/0031-9155/52/24/009>

Mukherjee, S., Hong, L., Deasy, J. O., & Zarepisheh, M. , Integrating soft and hard dose-volume constraints into hierarchical constrained IMRT optimization. *Medical Physics*, 47(2), 414–421, 2020. <https://doi.org/10.1002/mp.13908>

Murtagh, B. A., & Saunders, M. A. (1978). Large-scale linearly constrained optimization. *Mathematical Programming*, 14(1), 41–72. <https://doi.org/10.1007/BF01588950>

Nohadani, O., & Roy, A. (2017). Robust optimization with time-dependent uncertainty in radiation therapy. *IIE Transactions on Healthcare Systems Engineering*, 7(2), 81–92. <https://doi.org/10.1080/24725579.2017.1296907>

Rocha, H., Dias, J. M., Ferreira, B. C., & Lopes, M. C. , Discretization of optimal beamlet intensities in IMRT: A binary integer programming approach. *Mathematical and Computer Modelling*, 55(7–8), 1969–1980., 2012. <https://doi.org/10.1016/j.mcm.2011.11.056>

Romeijn, H. E., Ahuja, R. K., Dempsey, J. F., & Kumar, A. , A New Linear Programming Approach to Radiation Therapy Treatment Planning Problems. *Operations Research*, 54(2), 201–216, 2006. <https://doi.org/10.1287/opre.1050.0261>

Salari, E., Unkelbach, J., & Bortfeld, T. , A mathematical programming approach to the fractionation problem in chemoradiotherapy. *IIE Transactions on Healthcare Systems Engineering*, 5(2), 55–73, 2015. <https://doi.org/10.1080/19488300.2015.1017673>

Shepard, D. M., Earl, M. A., Li, X. A., Naqvi, S., & Yu, C. (2002). Direct aperture optimization: A turnkey solution for step-and-shoot IMRT. *Medical Physics*, 29(6), 1007–1018, 2002. <https://doi.org/10.1118/1.1477415>

ten Eikelder, S. C. M., Ajdari, A., Bortfeld, T., & den Hertog, D. (2021). Conic formulation of fluence map optimization problems. *Physics in Medicine & Biology*, 66(22), 225016, 2021. <https://doi.org/10.1088/1361-6560/ac2b82>

Thomas, E., Chapet, O., Kessler, M. L., Lawrence, T. S., & Ten Haken, R. K. , Benefit of using biologic parameters (EUD and NTCP) in IMRT optimization for treatment of intrahepatic tumors. *International Journal of Radiation Oncology*Biology*Physics*, 62(2), 571–578, 2005. <https://doi.org/10.1016/j.ijrobp.2005.02.033>

Witte, M. G., van der Geer, J., Schneider, C., Lebesque, J. V., Alber, M., & van Herk, M. , IMRT optimization including random and systematic geometric errors based on the expectation of TCP and NTCP. *Medical Physics*, 34(9), 3544–3555, 2007. <https://doi.org/10.1118/1.2760027>

Wu, Q., & Mohan, R. , Algorithms and functionality of an intensity modulated radiotherapy optimization system. *Medical Physics*, 27(4), 701–711, 2000. <https://doi.org/10.1118/1.598932>

Zaghian, M., Lim, G., Liu, W., & Mohan, R. , An Automatic Approach for Satisfying Dose-Volume Constraints in Linear Fluence Map Optimization for IMPT. *Journal of Cancer Therapy*, 05(02), 198–207, 2014. <https://doi.org/10.4236/jct.2014.52025>

Biographies

Atousa Arzanipour received her bachelor's and master's degrees in industrial engineering. In 2024, she earned a Master of Science degree from Iowa State University. She is currently a Ph.D. student at the Muma College of Business, University of South Florida. Her research interests lie in the areas of optimization and machine learning, and she has worked on numerous projects involving the application of optimization in healthcare systems, agricultural systems, and manufacturing. She received the Dean's Scholar Award from Iowa State University in 2021 and won the Best Poster Presentation Award in 2023 for her research titled "Data construction in a two-way table of means".

Dr. Majid Rafiee is an associate professor in the Industrial Engineering Department at Sharif University of Technology, where his academic interests span a range of interdisciplinary topics. His research focuses primarily on mathematical programming, robust and stochastic optimization, and decision-making under uncertainty. In addition to his expertise in operations research, he is also engaged in applied fields such as digital marketing, quality control, and healthcare systems engineering. Through his teaching and research, he aims to bridge the gap between theoretical models and real-world applications, contributing to both academic advancements and practical solutions in engineering and management systems.

Dr. Mehdi Mahnam is an Assistant Professor in the Department of Industrial and Systems Engineering at Isfahan University of Technology. In his research, he focuses on applying advanced optimization techniques to critical real-world problems such as healthcare systems, radiation therapy treatment planning, and large-scale production and scheduling challenges. His expertise encompasses integer programming, multi-objective optimization, and the development of efficient algorithms for complex operational issues. Through his scholarly work, he bridges theory and practice, contributing valuable insights toward the optimization of healthcare operations and industrial scheduling systems.